Optical Tolerancing for Diamond Turning Ogive Error

Mark Craig Gerchman

Rank Taylor Hobson Inc
Precision Park
Keene, New Hampshire 03431 USA

Abstract

This paper will investigate diamond turning ogive error. The equations that describe surfaces with ogive error will be derived from a simple Pythagorean model for tool offsets. The geometry of an ogive "sphere" will be reviewed and ogive form errors on aspheric surfaces will also be investigated. By considering the wavefront errors created by surfaces with ogive error the implications for optical tolerancing will be examined.

Introduction

Recent developments in diamond turning lathes have had a significant effect on the quality of machined optical surfaces.[1] With these developments in lathe accuracies other conditions, unrelated to machine tool geometry, dominate the causes of surface form errors. These conditions include improper component mounting, cutting tool conditions and dynamic machining effects.[2] For further significant improvements to be made in the quality of directly machined surfaces these conditions will need to be examined, understood, and corrected. This paper will examine one aspect of these conditions and model its effect on the machined optical surface. This aspect is the problem of diamond machining with tool offsets and its effect on surface distortion known as ogive error.

Ogive Geometrical Model

The use of the term ogive error to describe the geometry created when diamond machining with tool offsets is particularly descriptive. The term ogive is usually associated with a gothic architectural design form. In use since the eleventh century, the pointed ogival style is prominent in most European "high" architecture. The constructional aspects of an ogive form are shown in Figure 1. The basis of an ogive form is the generating curve, usually a circular arc section. To create the ogive figure this generating curve is placed symmetrically about the figure's axis. The ogive figure's degree of "pointedness" depends on the amount of offset between the generating curve vertex and the axis of symmetry. Note that the vertex can lie on either side of the axis creating both open and closed ogive figures. This is analogous to what can occur in two axis diamond machining when the cutting tool is offset from the centerline of the rotating workpiece.

In two axis orthogonal diamond machining the diamond tool is moved relative to a rotating workpiece in a coordinated motion along two perpendicular axes to describe a generating curve in space. If at the vertex of the generating curve the tool is not coincident with the rotational axis of the workpiece, then a tool offset is present. A machined surface generated with a tool offset is described as an ogive surface of revolution. This description will serve as the physical basis for this model of diamond turning ogive error. To simplify this model the following assumptions are made: the coordinated motion of the tool in describing the generating curve is perfect, the rotating workpiece and the centerline for the generating figure are parallel, tool radius effects are compensated, and no dynamic machining effects exist.

Figure 2 shows this Pythagorean model for ogive geometry. The vertex of the generating curve is shown offset from the centerline of a coordinate system that defines the rotating workpiece by the amounts δx and δy. The distance from the rotating centerline to a cutting point on the curve and surface, ρ, is the Pythagorean sum of the tool offsets and the radial distance, x, on the generating curve.

$$\rho = \sqrt{(x + \delta x)^2 + \delta y^2} \tag{1}$$

This equation can be inverted to yield the radial coordinate in the machining plane as a function of the rotational coordinate.

$$x(\rho) = (\rho^2 - \delta y^2)^{1/2} - \delta x \tag{2}$$

If the generating curve is represented as a sagittal function of the radial coordinate, i.e. $z = z(x)$, then the ogive surface of revolution is described by a direct substitution with Equation 2.

$$z = z(x) = z([\rho^2 - \delta y^2]^{1/2} - \delta x) \tag{3}$$

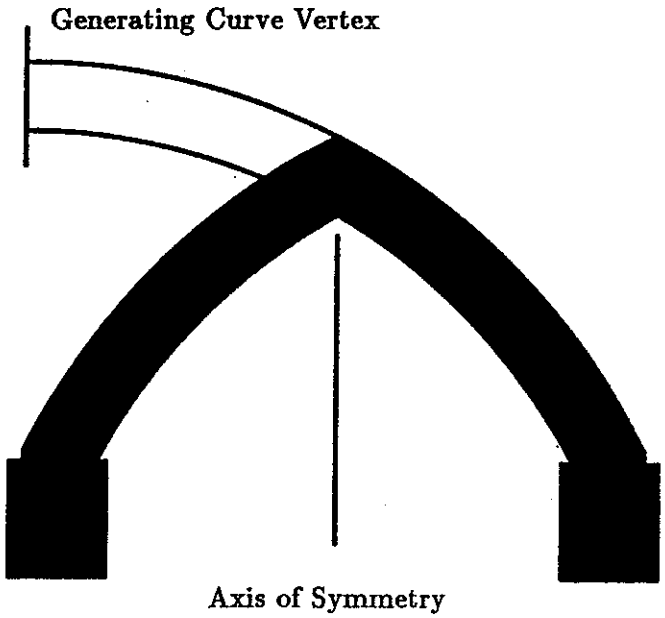

Figure 1 - Ogive Arch

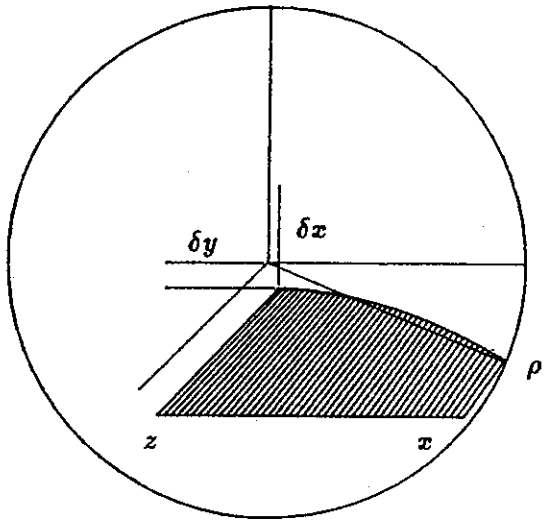

Figure 2 - Ogive Geometry

An Example: The Ogive "Sphere"

Before applying this Pythagorean representation for ogive error to general aspheric surfaces we will investigate the case of an ogive "sphere". This case is particularly important because by evaluating a "sphere" with ogive error the amount of tool offset present can be calculated and corrected to a degree.[3] The generating curve for a sphere is a circular section. Using the common sagitta equation for the section of a circle with radius, r, a direct substitution from Equation 3 can be made to yield the exact equation for an ogive "sphere".

$$z = z(x) = r - \sqrt{r^2 - x^2} = z(\rho) = r - \sqrt{r^2 - [(\rho^2 - \delta y^2)^{1/2} - \delta x]^2} \tag{4}$$

It should be noted that a tool offset δx enters into this equation in a very different fashion from a tool offset δy. Assuming that the rotational coordinate is much greater than the tool offsets, i.e. $\rho \gg \delta x, \delta y$, then a binomial expansion of Equation 2 can be made.

$$x = x(\rho) = \rho - \frac{\delta y^2}{2r} - \frac{\delta y^4}{8r^3} - \cdots - \delta x \tag{5}$$

This assumption will be true over the majority of the surface except at the center of rotation. At the center of rotation the radius of the diamond tool will dominate the geometry in the presence of a δx offset and a cosmetic

defect will result from a δy offset. Over the remainder of the surface, Equation 5 shows that the ogive figure is influenced less by δy offsets than δx offsets because of the the relative strength of the terms. This is why it is possible to set the height of diamond tools with the aid of a microscope and an interferometer is needed to reduce x offsets. It should also be noted that δy is present in the equation only in an even power expansion unlike δx which is sign dependent. Therefore, one can not distinguish from the macroscopic ogive surface if a tool offset in the y direction places the tool above or below rotational centerline, while it is relatively easy to access which side of the rotational axis the vertex of the generating curve lies. If we neglect terms with higher order offset dependencies, then Equation 5 reduces to an expression similar to a differential.

$$x = x(\rho) \approx \rho - \delta x \tag{6}$$

Using this simplification, the equation for the sagittal difference between this ogive "sphere" and the same sphere without an offset can be given.

$$\delta z = z(\rho, \delta x = 0) - z(\rho) = \sqrt{r^2 - (\rho - \delta x)^2} - \sqrt{r^2 - \rho^2} \tag{7}$$

If the following further assumption is made that the radius of the sphere is much larger than the surface aperture, $r \gg \rho$, then these radicals can also be binomially expanded.

$$\delta z \approx \frac{\rho^2}{2r} - \frac{(\rho - \delta x)^2}{2r} = \frac{\rho \delta x}{r} - \frac{\delta x^2}{2r} \tag{8}$$

Continuing to neglect terms with higher order offset dependences yields the following sagitta difference.

$$\delta z \approx \frac{\rho \delta x}{r} \tag{9}$$

An ogive "sphere" therefore has a conical error profile in the rotational coordinate, ρ. In the interferometric evaluation of such a surface, the center of the reference wavefront can be displaced so that the conical error appears tilted. Proper selection of this displacement permits the optical path difference to be minimized between the center of the figure and one edge and yielding twice the sagitta error between the center and the opposite edge. An inversion of Equation 9 along with this factor of two from the tilted profile can be used to determine the δx offset from an interferometric determination of the ogive "sphere".

$$\delta x \approx \frac{r \delta z}{2\rho} \tag{10}$$

Figure 3 shows an example of this relationship. This figure represents a synthetic interferogram generated from a ray-trace algorithm with rays traced off the following surface. The surface has a radius of curvature of 500mm (20 inches), an aperture of 50mm (2 inches), a δx offset of 12.5 μm (0.000,5 inches) and no δy offset. Rays were traced off this surface using the exact representation of the ogive surface as given in Equation 4. By the proper displacement of the reference spherical wavefront center, to minimize the optical path difference between the center and left-hand edge, the expected four fringes @ 632.8nm or 1.25μm (0.000,05 inches) of δz are observed.

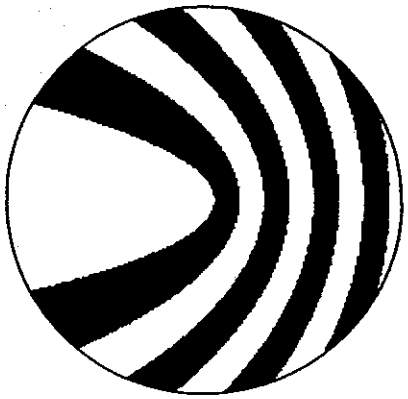

radius of curvature r	500mm
aperture diameter 2ρ	50mm
tool offset δx	12.5μm
tool offset δy	0.0μm
sagitta error δz	1.25μm

Figure 3 - Synthetic Interferogram for an Ogive "Sphere"

Ogive Form Errors On Aspheric Surfaces

The most common sagitta equation used for the representation of aspheric optical surfaces is the following.

$$z = z(x) = \frac{cx^2}{1 + \sqrt{1 - (k+1)c^2x^2}} + a_1x + a_2x^2 + a_3x^3 + a_4x^4 \cdots \tag{11}$$

This equation defines a conic surface of revolution modified by simple polynomial terms. With a direct substitution from Equation 2, the ogive form for the aspheric surface is given. By ray-tracing using this exact representation, optical tolerancing for ogive errors can be obtained. A more insightful investigation of optical tolerancing can be accomplished by using the approximations of Equation 6. Considering this expression to be an exact differential, a simplified representation of the sagitta difference as a product of the derivative of the aspheric generating curve and the δx offset is possible.

$$\delta z \approx \frac{\partial z}{\partial x}\delta x = \left[\frac{cx}{\sqrt{1 - (k+1)c^2x^2}} + a_1 + 2a_2x + 3a_3x^2 + 4a_4x^3 + \cdots\right]\delta x \tag{12}$$

Ogive form error is therefore sensitive to the slope of the generating equation and not to the total surface sagitta. The slope can be the result of either the optical speed of the surface or higher order polynomial terms. Certain observations can be made based on this simplification. A linear axicon, i.e. a cone shaped surface, will not suffer from ogive error but only an axial displacement of the surface. The ogive error for a parabolic surface will have a linear radial dependence. This is consistent with the approximations made for the case of an ogive "sphere".

Equation 12 has other interesting implications. This equation has the exact form as the radial shearing interferometer equation where the differential, δx, is the displacement between the radially sheared wavefronts. [4] Although radial shearing interferometers are often used to evaluate aspheric surfaces, the similarity between the ogive surface and the testing technique can make the proper interpretation of the interference pattern difficult. It is very important when evaluating diamond turned surfaces by radial shearing interferometry to consider this effect.

Tolerancing Considerations and Ogive Error

The relationship between surface distortions in an optical system and image quality is complex. Factors such as surrounding media, surface proximity to stops and pupils, field angle considerations, and wavefront obliquity all effect how surface distortions influences image quality. In a rigorous sense the tolerancing of optical surfaces to satisfy a system's imaging requirement must take into account these factors and more. To tolerance surfaces with ogive error, ray-tracing can be used in conjunction with this Pythagorean model to provide exact simulations. Tolerancing considerations of ogive error can be investigated by examining the influence on image quality of wavefronts aberrated by by ogive surfaces.

Ogive aberrated wavefronts would be radially symmetric and related to the derivative of the defining aspheric generating curve. Wavefronts composed of simple radial dependent terms can be used to compare the effects of different order aspheric terms on image quality. The wavefront error, δw, in the exit pupil can be defined as a coefficient related to the severity of the ogive error, α_n, times the radial position raised to an appropriate power.

$$\delta w = \alpha_n \rho^n \tag{13}$$

When these wavefront errors are small the Strehl intensity for such a system will be degraded by the square of the root-mean-square departure from a reference spherical wavefront. A measure of the sensitivity of these wavefront errors can be obtained by comparing *rms* values for wavefronts with different radial dependencies but with the same peak-to-valley error. The *rms* values for these wavefronts can be calculated from the following definition.

$$rms = \left[\frac{\int_0^{2\pi}\int_0^{\rho'}\left[\delta w(\rho) + \alpha_0 + \alpha_2\rho^2\right]^2 \rho\partial\rho\partial\vartheta}{\int_0^{2\pi}\int_0^{\rho'}\rho\partial\rho\partial\vartheta}\right]^{1/2} \tag{14}$$

In Equation 14 the *rms* value is calculated based on the wavefront error, δw, a best fit piston term, α_0, and a best fit defocus term, α_2. In the interest of comparison, the analysis can be simplified by considering the integration over a unit circle exit pupil (i.e. $\rho' = 1$) and with an unfocused peak-to-valley wavefront error of unity (i.e. $\alpha_n = 1$).

$$rms = \left[\frac{\int_0^{2\pi} \int_0^1 \left(\rho^n + \alpha_0 + \alpha_2 \rho^2\right)^2 \rho \partial \rho \partial \vartheta}{\int_0^{2\pi} \int_0^1 \rho \partial \rho \partial \vartheta} \right]^{1/2} \tag{15}$$

After integration the *rms* can be explicitly expressed.

$$rms = \left[\frac{1}{n+1} + \alpha_0^2 + \frac{\alpha_2^2}{3} + \frac{4\alpha_0}{n+2} + \frac{4\alpha_2}{n+4} + \alpha_0 \alpha_2 \right]^{1/2} \tag{16}$$

Partial derivatives of equation 16 can be taken and optimized values for piston, α_0, and defocus, α_2, determined algebraically from a least squares reduction.

$$\alpha_0 = 4 \left[\frac{3}{n+4} - \frac{2}{n+2} \right] \tag{17}$$

$$\alpha_2 = 12 \left[\frac{1}{n+2} - \frac{2}{n+4} \right] \tag{18}$$

By substituting these optimized values for piston and defocus into Equation 16, values the peak-to-valley and *rms* wavefront distortions can be calculated. These results are summarized in the table below.

Wavefront Data for Different Polynomial Terms

exponent	α_0	α_2	P-V	RMS
1	-0.266667	-0.800000	0.312500	0.047140
2	0.000000	-1.000000	0.000000	0.000000
3	0.114286	-1.028571	0.161213	0.042857
4	0.166667	-1.000000	0.250000	0.074536
5	0.190476	-0.952381	0.347910	0.097202
6	0.200000	-0.900000	0.428634	0.113389
7	0.202020	-0.848485	0.495347	0.124994
8	0.200000	-0.800000	0.550882	0.133333
9	0.195804	-0.755245	0.597515	0.139317
10	0.190476	-0.714286	0.637022	0.143577

Here is an example of how the data in this table can be used to assist in optical tolerancing ogive error. Consider the variations in wavefront *rms* values for aberrated wavefront caused by a parabolic reflector. If the wavefront error is aberrated due to ogive error the power dependence will be first-order. If the wavefront error is similar to third-order spherical aberration the power dependence will be fourth-order. From the table above it can be seen that the ogive error effect on *rms* will be almost half the effect of third-order spherical aberration (i.e. 0.047140 to 0.074536). The Strehl ratio, and hence image quality, of a system will be substantially better for the ogive paraboloid then the spherically aberrated paraboloid. Optical tolerancing of the ogive surface in this instance can be considerably loosened when compared with a model for surface distortion that is spherically aberrated. Figure 4 shows synthetic interferograms for these wavefronts.

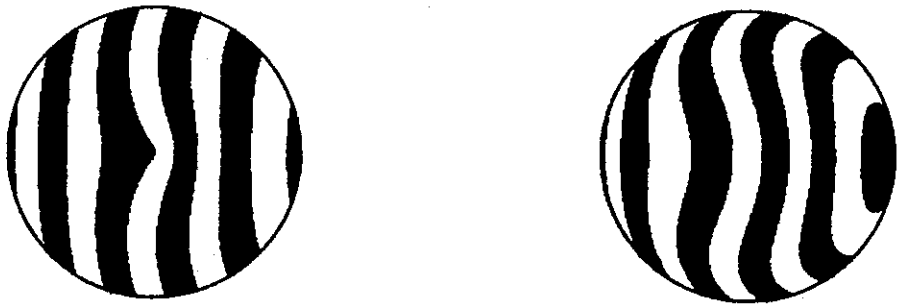

Ogive Wavefront **3rd Order Spherically Aberrated Wavefront**

Figure 4 - Synthetic Interferogram for Aberrated Wavefronts

Conclusion

This paper has shown how diamond machining ogive error can be based on a Pythagorean model for tool offset. Using this model the form error of an ogive "sphere" and asphere have been examined. It has been shown that optical tolerancing for ogive error will be dependent on the derivative of the aspheric surface form and has a significant effect on optical tolerancing.

References

[1] "The results of cutting tests performed on a sub-micro-inch resolution lathe", Youden, David H., Proc. American Society for Precision Engineering 3rd Annual Precision Engineering Conference 1988.

[2] "Factors governing form accuracy in diamond machine components", Myler, J.K. and D.A. Page, SPIE Proc.915 Recent Developments in Infrared Components and Subsystems, ed. C.T. Elliott, 1988.

[3] "Diamond-turning tool setting by interference analysis", Rasnick,W.H. and R.C. Yoder, US Govt. Contract W-7405-ENG-26, available from the National Technical Information Service Pub. No. PB81970767, 1980.

[4] "Mathematical interpretation of radial shearing interferometers", Malacara, Daniel, Applied Optics, Volume 13, No. 8, 1974.